Electronic structure of the mixed valence system $(YM)_2BaNiO_5$ $(M=Ca,Sr)$

P. Novák
Institute of Physics, Academy of Sciences of the Czech Republic, Cukrovarnická 10, 162 53 Praha 6, Czech Republic

F. Boucher and P. Gressier
Institut des Matériaux Jean Rouxel, UMR 6502 CNRS-Université de Nantes, Boîte Postale 32229, 44322 Nantes Cedex 3, France

P. Blaha and K. Schwarz
Institute of Physical and Theoretical Chemistry, TU Vienna, Getreidemarkt 9, A-1060 Vienna, Austria

(Received 18 December 2000; published 25 May 2001)

Electronic structure of the system $Y_{2-x}M_xBaNiO_5$ $(M=Ca,Sr)$ was calculated for $x=0$, 0.2, and 0.5 using the full-potential linearized augmented-plane-wave method. To describe the exchange and correlation the local spin-density approximation (LSDA), generalized-gradient approximation (GGA), and two versions of the LSDA+U method were employed. Independently of the method used, the ground state of the parent compound corresponds to an antiferromagnetic insulator. The gap as obtained by LSDA and GGA is smaller than the experimental gap, while LSDA+U methods yield the correct value. To calculate the electronic structure in the mixed-valence region $(x\neq 0)$ the virtual-crystal approach was used. The ground state of the system is still antiferromagnetic, but a finite density of states appears at the Fermi level. The oxygen *K*-edge x-ray absorption spectra calculated using the LSDA+U methods agree well with the experiment, in particular, the appearance of an additional peak when Y^{3+} is substituted by the M^{2+} cation is correctly described.

DOI: 10.1103/PhysRevB.63.235114 PACS number(s): 71.28.+d, 71.15.−m

I. INTRODUCTION

There are several reasons for which the calculation of the electronic structure of $Y_{2-x}M_xBaNiO_5$ $(M=Ca,Sr)$ system is interesting. The parent compound $x=0$ is a quasi-one-dimensional antiferromagnet with a charge gap ≈ 2.3 eV.[1] Its electronic structure was first calculated by Mattheiss,[2] who used the full-potential linearized augmented-plane-wave method (FPLAPW), but his calculation was nonmagnetic. The more recent calculation of Maiti and Sarma[1] is spin-polarized, but uses the muffin-tin approximation for the potential. In both calculations a metalliclike ground state was obtained in clear conflict with the reality. As we shall show, the full potential, spin-polarized calculation yields a correct result—ground state of the parent compound corresponds to an antiferromagnetic insulator. The doping by a divalent cation *M* adds charge carriers in the system and changes markedly its physical properties.[3] In particular a spin-density modulation appears, which resembles those seen in the metallic cuprates. They were interpreted as antiferromagnetic droplets, which develop around the substitution site in the singlet ground state of a quantum-spin liquid.[4] The interpretation is based on an assumption that the holes induced by the doping reside in the oxygen *p* states. It is beyond the scope of the present band-structure calculation to treat the local perturbations of electronic structure around the impurity, however, the character of the states on the Fermi level is one of its results. The parent compound exhibits the dc resistivity ρ of the usual activated form with strongly one-dimensional (1D) character.[3] Ca doping greatly lowers ρ, while preserving its 1D character. The temperature dependence of ρ for $x\neq 0$ is consistent with the variable-range-hopping mechanism, indicating that the added carriers have a localized, rather than metallic character.[3]

Another intriguing feature of $Y_{2-x}M_xBaNiO_5$ system is the anomalous dependence of the lattice parameters on the concentration of *M*. Though the ionic radii of Ca^{2+} and Sr^{2+} are larger than the radius of Y^{3+} ion, the parameter *c* decreases with increasing *x*. For $M=Ca$, not only *c* but also *a* and the unit-cell volume decrease when the Ca concentration increases.[5] Evidently, the origin of this anomaly is to be sought in the electronic structure.

In this paper we present the results of spin-polarized calculations using the FPLAPW method as implemented in the WIEN package.[6] In addition to the local spin-density approximation (LSDA) and the generalized-gradient approximation (GGA) the LSDA+U method, which was recently added to the WIEN program,[7] is used. To compare the quasi-one-dimensional antiferromagnet with a similar three-dimensional one, calculations with analogous input parameters (number of *k* points, number of basis functions, radii of atomic spheres, etc.) were performed for NiO. To estimate the strength of the antiferromagnetic exchange we also made nonmagnetic calculations with the LDA and GGA potentials.

II. COMPUTATIONAL DETAILS

The crystal structure of the parent compound Y_2BaNiO_5 was first investigated by Amador *et al.*,[8] Buttrey *et al.*,[9] and Müller-Buschbaum and Schlütter.[10] It belongs to the R_2BaNiO_5 (*R*, rare earth) family of oxides described first by Schiffler and Müller-Buschbaum.[11] The Y_2BaNiO_5 compound crystallizes in a body-centered orthorhombic cell with the space group *Immm* ($a=1.13337$ nm, $b=0.57627$ nm, $c=0.37622$ nm).[12] The structure is built from the chains of NiO_6 octahedra, sharing corners along the *c* axis. The octahedra are strongly compressed along this axis with two short Ni-O1 distances (0.1881 nm) and four longer

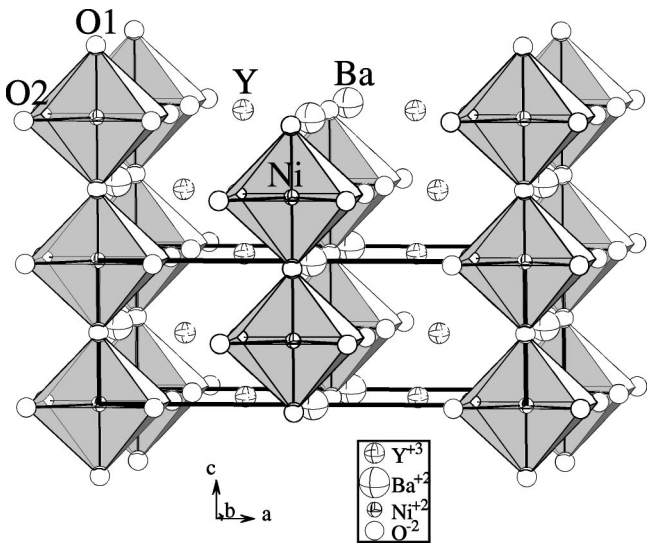

FIG. 1. Orthorhombic unit cell of Y_2BaNiO_5.

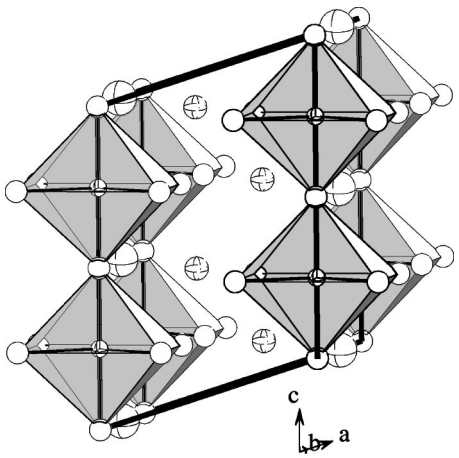

FIG. 2. Triclinic unit cell of antiferromagnetic Y_2BaNiO_5, which was used in the present calculations. For the definition of the atoms see Fig. 1.

Ni-O2 distances (0.2186 nm) in the basal plane. The chains are separated by Y^{3+} and Ba^{2+} cations. As the Ni-Ni interchain interaction is negligible, the compound exhibits a pseudo 1D magnetic behavior.

For the spin-polarized calculations, in order to describe the antiferromagnetic ordering in the chain, a larger unit cell must be considered. Maiti and Sarma[1] made an obvious choice—the primitive orthorhombic cell was doubled along the *c* axis. The centering is then lost and the structure can be described with the space group $Pmmn$. The unit cell contains 36 atoms (four formula units) and there are two Ni-O-Ni chains, which are not related by any symmetry operation (Fig. 1). Corresponding calculaton using the FPLAPW code would be very demanding on the computer memory and power, and for this reason we made a different choice. Taking into account that the magnetic interchain interaction is insignificant, we used a twice smaller triclinic cell with the space group $P1$, containing only single Ni-O-Ni chain in the unit cell (18 atoms). The cell is obtained from the original, body-centered one by a transformation

$$\vec{a}' = \frac{1}{2}\vec{a} - \frac{1}{2}\vec{b} + \frac{1}{2}\vec{c}, \quad \vec{b}' = \vec{b}, \quad \vec{c}' = 2\vec{c}. \tag{1}$$

This triclinic cell allows to keep the symmetry translation related to the original body centering. It also has an additional advantage—because there is only one Ni-O-Ni chain the problem of the mutual orientation of spins in different chains does not arise. This is in accord with the quasi-1D character of the magnetism in the system in question. The cell is displayed in Fig. 2 and the atomic co-ordinates and the cell parameters a,b,c may be found in Ref. 12.

In the LSDA and LSDA+U calculations the Perdew and Wang parametrization[13] of the exchange-correlation potential was adopted, while the GGA potential was that of Perdew, Burke, and Ernzerhof.[14] In all cases the calculation was performed at 48*k* points of the full Brillouin zone and the number of basis functions was ≈ 1800. We tested that increasing these parameters has only a marginal effect on the results. The radii of atomic spheres were taken as (in atomic units) 2, 2, 1.9, and 1.65 for Y, Ba, Ni, and O, respectively. Note that because of the short Ni-O distance along the c' axis the radii of Ni and O are smaller than in standard calculations of other Ni oxides.

A. LSDA+U

The LSDA+U method was introduced by Anisimov *et al.*[15] in order to improve the description of the systems with a strong electron correlation. To this end an orbitally dependent potential is introduced for the chosen set of electron states, which in our case are $3d$ states of Ni. In an early version ($LSDA+U^{DFT}$ in what follows), the additional potential, which mimicks the Hubbard term, is zero when averaged over the chosen set of states and this method is thus as close as possible to the original (density-functional theory) DFT-LSDA. In a later version[16] the LSDA interaction is subtracted and replaced by a Hartree-Fock form for the electron-electron interaction in the spherically symmetrical atom. This has an advantage that the self-interaction of the electrons is approximatively removed and for this reason, in what follows we call this version $LSDA+U^{SIC}$. The difference between the two versions is clearly seen if the density matrix is diagonal and the terms proportional to J are neglected (i.e., only the Hartree term is considered). The additional potentials $V_m^{(DFT)}$, $V_m^{(SIC)}$ are then

$$V_m^{(DFT)} = U(\langle n^\sigma \rangle - n_m), \quad V_m^{(SIC)} = U\left(\frac{1}{2} - n_m\right), \tag{2}$$

where $\langle n^\sigma \rangle$ is the number of electrons averaged over the five $3d$ states of Ni with spin σ. At present the $LSDA+U^{SIC}$ is almost exclusively used. However, the form of the potential, which is subtracted (''double-counting correction'') is taken from the spherically symmetrical atoms and it is not clear to which extent its application in the full-potential methods is justified. To our knowledge $LSDA+U^{DFT}$ method was not applied before this work in the rotationally invariant form, which does not make an assumption of the density matrix

being diagonal. In the present paper the results obtained by both LSDA+U variants are compared. We note that the experience with LSDA+U in the methods using the full potential is very limited and the only other implementation in the FPLAPW program[18] employs its LSDA+U^{SIC} version.

B. Mixed valence region

The substitution of M in $Y_{2-x}M_xBaNiO_5$ is limited to $x<0.5$ and the M atoms are distributed randomly. In this situation, in order to treat the substitution, the supercell method is usually used. However, in the present spin-polarized calculations the unit cell of the parent compound comprises 18 atoms, all of which are inequivalent. To perform the supercell calculation with the FPLAPW method would then be costly and for small x, nearly impossible. To overcome this difficulty, we used the fact that as far as the chemical bonding is concerned, Y and M behave similarly. The substitution can be then treated by a ''virtual crystal'' method, successfully applied by Pickett and Singh to substituted manganites.[19] In the virtual-crystal method the electron holes, number of which is equal to the number of M^{2+} cations, are introduced by reducing the number of valence electrons per unit cell by Nx, where N is the number of formula units in the unit cell. To keep the system electrically neutral the Y atoms with atomic number $Z=39$ are replaced by ''virtual'' atoms with fractional atomic number $Z=39-x/2$. The system retains original periodicity, so that any effect of the disorder is suppressed. To check the applicability of the method we performed for $Y_{1.5}Ca_{0.5}BaNiO_5$ two calculations—in the first one the virtual atoms with $Z=38.75$ were introduced instead of all Y atoms, while in the second calculation one of the four Y in the unit cell was replaced by Ca (LSDA exchange correlation potential was employed). The calculations yielded very similar results, e.g., the Ni spin changes by less than 0.5% and there is only small change in the density of states (Fig. 3). We conclude therefore that if the effect of disorder is neglected, the substitution of yttrium by a divalent cation in Y_2BaNiO_5 could be well accounted for by the virtual-crystal method and we employed this method to obtain the results described below.

In order to isolate the effect of the M substitution itself on the electronic structure, we used in calculations for all x the crystal structure of the parent compound. Recently new crystal structure data for several x and $M=$Ca became available.[5] To see how the change of crystal structure influences the results, the LSDA calculation for $x=0.2$ was repeated using the crystal structure of $x=0.18$ compound as given in Ref. 5. The differences between the two calculations are very small—the change in Ni spin is 0.7%, the difference of energy between antiferromagnetic and nonmagnetic state is virtually the same and also the density of states is only slightly modified (Fig. 4).

C. Parameters U and J

In most of the calculations we used the values $U=8$ eV, $J=0.95$ eV appropriate for the nickel monoxide.[17] To see how the magnitudes of parameters U and J influence the results of the LDA+U method, for $x=0.2$ the calculations with scaled U and J were performed. When U and J are reduced the results of the calculation change smoothly as seen in Fig. 5, where the magnitude of Ni spin and the value Δ of the gap between the group of states on the Fermi energy and the nearest higher states are plotted as functions of $U/U(\mathrm{NiO})=J/J(\mathrm{NiO})$.

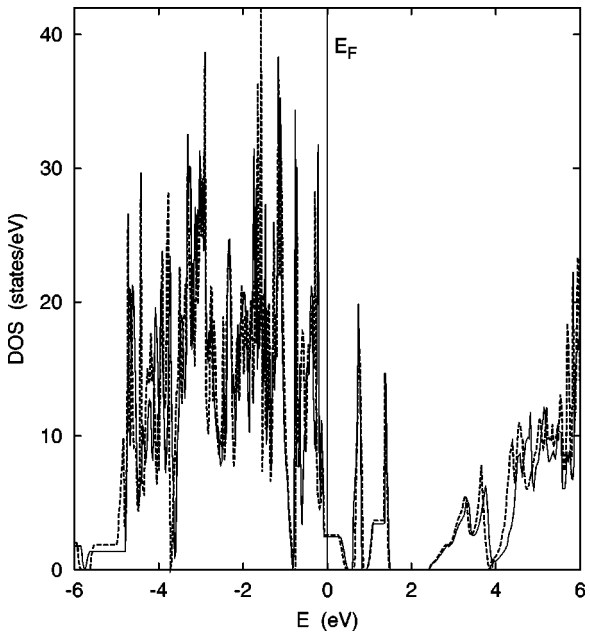

FIG. 3. Comparison of the total density of states for $Y_{1.5}Ca_{0.5}BaNiO_5$ calculated by replacing one Y atom in the unit cell by Ca (full curve) and by the ''virtual-crystal'' method (dashed curve).

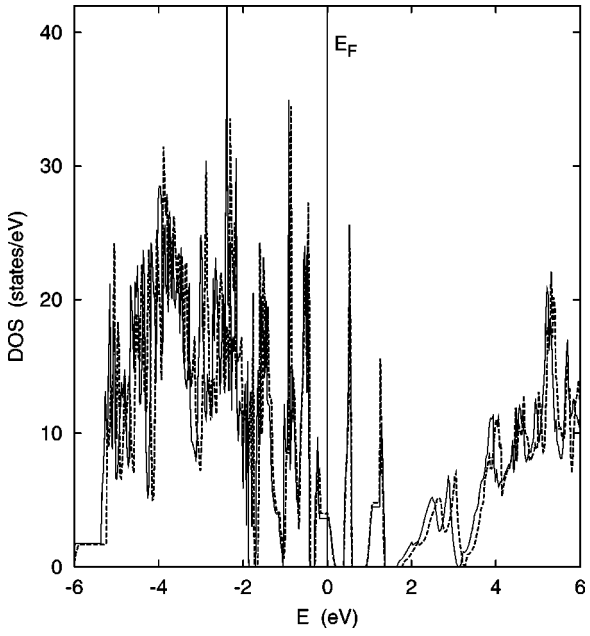

FIG. 4. Comparison of the total density of states for $Y_{1.8}M_{0.2}BaNiO_5$ calculated with the crystal structure of the parent compound (full curve) and with the crystal data of Ref. 5 for $M=$Ca, $x=0.18$ (dashed curve).

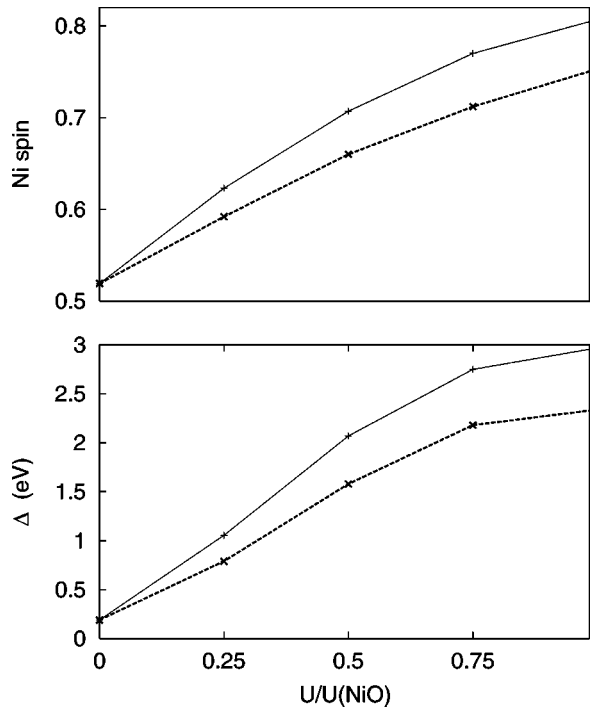

FIG. 5. The spin of Ni (upper panel) and the energy difference Δ between the group of states on the Fermi energy and the nearest higher states (lower panel) as functions of $U/U(\mathrm{NiO})=J/J(\mathrm{NiO})$. Full and dotted curves correspond to the SIC and DFT version of LSDA+U, respectively. The content of the substitution is $x=0.2$.

III. RESULTS AND DISCUSSION

A. Y_2BaNiO_5

The first important result obtained for the parent compound is that the antiferromagnetic interaction opens the gap, making the ground state insulatorlike. The gap amounts to 0.3 eV for the LSDA and increases to 2.8 eV for the LSDA+U^{SIC} method. The most important data are summarized in Table I where, for comparison, we include also the data obtained for NiO. The magnitude of the gap as calculated by LSDA+U^{DFT} is in good agreement with the experiment, while the larger value obtained by LSDA+U^{SIC} indicates that for this method U should be reduced by $\approx 20-30$ % in order to obtain an agreement with the experiment. LSDA yields the gap that is almost an order of magnitude smaller than the experimental value. The improved value obtained by the GGA method, though still insufficient, is expected as GGA is better suited for treatment of the systems with strong electron correlation.

TABLE I. Energy gap Δ (eV), spin of Ni, spin of O2 in Y_2BaNiO_5 and the energy difference δ per formula unit (eV) between nonmagnetic and antiferromagnetic states. In NiO the spin of oxygen is zero, similar to that of O1 in Y_2BaNiO_5.

	Y_2BaNiO_5				NiO		
Method	Δ	S(Ni)	S(O2)	δ	Δ	S(Ni)	δ
LSDA	0.3	0.647	0.038	0.274	0.4	0.605	0.177
GGA	0.8	0.702	0.036	0.454	0.9	0.689	0.379
LSDA+U^{DFT}	2.2	0.807	0.021		2.6	0.847	
LSDA+U^{SIC}	2.8	0.846	0.020		3.3	0.878	

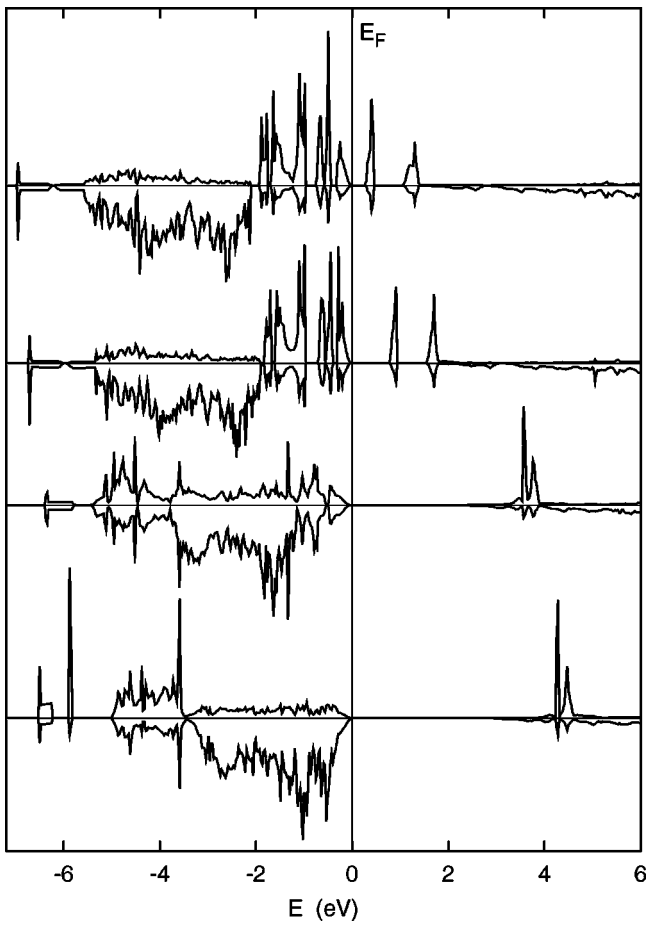

FIG. 6. Y_2BaNiO_5. Comparison of Ni and O density of states as obtained by different methods. To obtain the curves, the projected densities of states of all Ni and oxygen atoms in the unit cell were summed. The oxygen DOS is plotted with the negative sign. The four cases correspond to LSDA (curves at the top), then follows GGA, LSDA+U^{DFT}, and LSDA+U^{SIC} (curves at the bottom).

The second important result is that the character of states just below the Fermi energy depends strongly on the method used. While for LSDA and GGA $3d$ states of Ni prevail, in LSDA+U^{SIC} the O($2p$) states dominate and LSDA+U^{DFT} gives $\approx 1:1$ ratio for Ni($3d$) and O($2p$) character. The difference between LSDA and GGA on the one side and LSDA +U on the other side arises from the fact that the additional LSDA+U potential lowers the energy of the majority $3d$ states of Ni and increases the energy of minority ones, pushing thus the Ni($3d$) states apart from the Fermi level. To illustrate the situation, Ni- and O-projected density of states as obtained in the four methods are compared in Fig. 6. LSDA and GGA thus yield the density of states characteristic for the Mott-Hubbard insulator, contrary to LSDA+U^{SIC} which results in a charge-transfer-insulating ground state. For all four methods, however, the two narrow bands found above the Fermi level (Fig. 6) have similar character. They correspond to the σ^*, Ni($3d_{z^2}$)$-$O($2p$), and Ni($3d_{x^2-y^2}$)

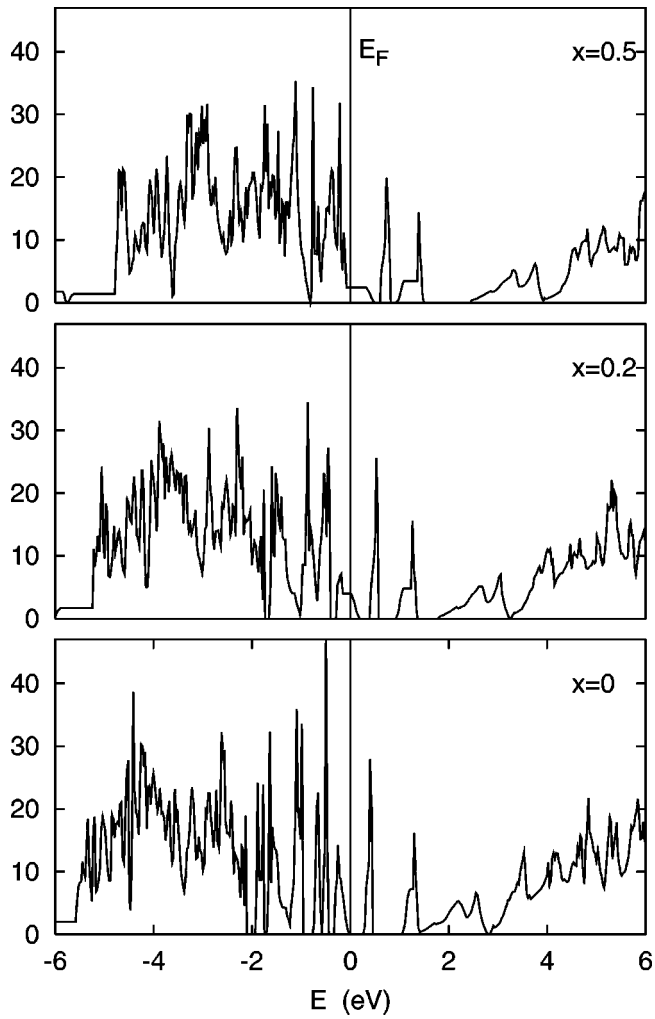

FIG. 7. LSDA method. Total DOS in states/eV of $Y_{2-x}M_xBaNiO_5$ for $x=0$, 0.2, and 0.5.

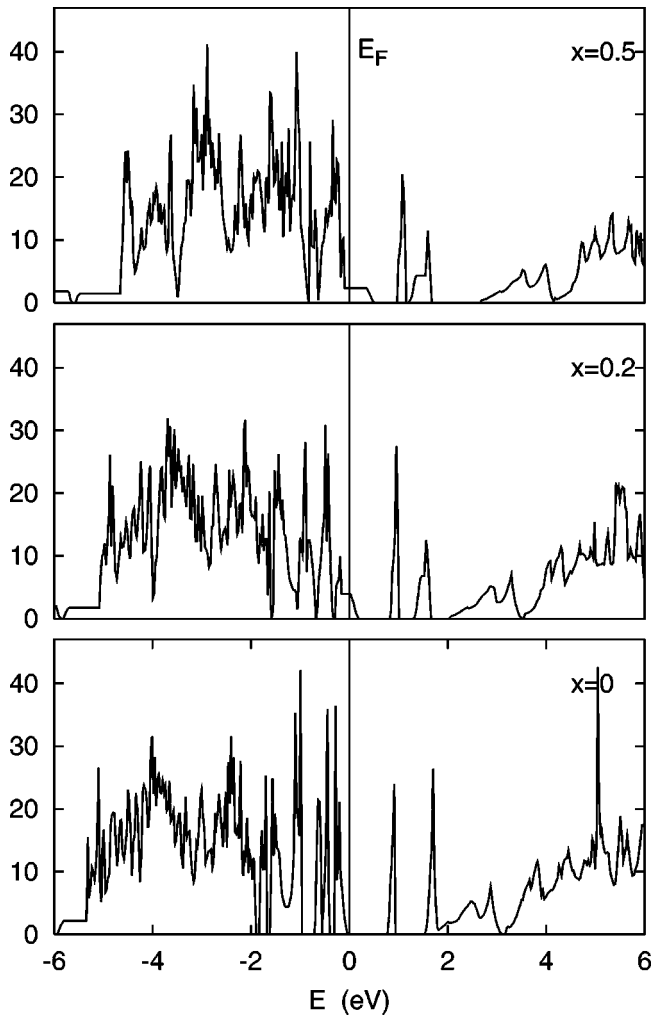

FIG. 8. Same as Fig. 7 but for the GGA method.

$-O(2p)$ spin-minority bands. The degree of localization of corresponding states does depend on the method, however.

The energy δ gained by an antiferromagnetic ordering is larger in Y_2BaNiO_5 than in NiO, suggesting that the Ni-Ni exchange interaction in the chain is very strong, presumably because of the anomalously short Ni-O distances.

B. Mixed valence region

The calculations were performed for two concentrations of M, $x=0.2$ and $x=0.5$, using the four methods described above. In all cases the nonzero density of states appears at the Fermi level and the system becomes metalliclike. This disagrees with the temperature dependence of the dc resistivity,[3] the conflict is not surprising, however. In a 1D material the disorder induced by even a small doping leads to a localization. As mentioned above, in our calculation this disorder is neglected.

As in the parent compound the character of the states in the vicinity of E_F strongly depends on the method used. In Figs. 7–10 the evolution of density of states (DOS) with increasing x is displayed for the four methods. The character of states that are close to the Fermi level is similar to that in the parent compound—for LSDA and GGA the $3d$ Ni states prevail, for LSDA+U^{SIC} the O $2p$ states dominate, while LSDA+U^{DFT} method keeps $\approx 1{:}1$ ratio of the Ni($3d$) and O($2p$) states.

The spin of Ni decreases with increasing x and also the difference δ between the total energy of antiferromagnetic and paramagnetic states decreases (Fig. 11). This difference was calculated only for LSDA and GGA, as in LSDA+U methods the exchange polarization is lost in the paramagnetic state, which prevents any reliable comparison. The decrease of δ may be connected with the existence of the ferromagnetic double exchange in the substituted systems—there is a gain in the kinetic energy of the electron holes if the Ni spins are parallel.

In order to understand the anomalous dependence of the unit-cell parameters on x, the character of the bands that cross the Fermi level must be investigated. We performed a detailed analysis for the $Y_{1.8}M_{0.2}BaNiO_5$ system with the band structure calculated by the LSDA+U^{DFT} method. As seen in Fig. 12 there is single band crossing E_F. Using the density of states projected on the atomic spheres, we determined that for $E=E_F$ this band has 49% of Ni spin-up $3d_{z^2}$,

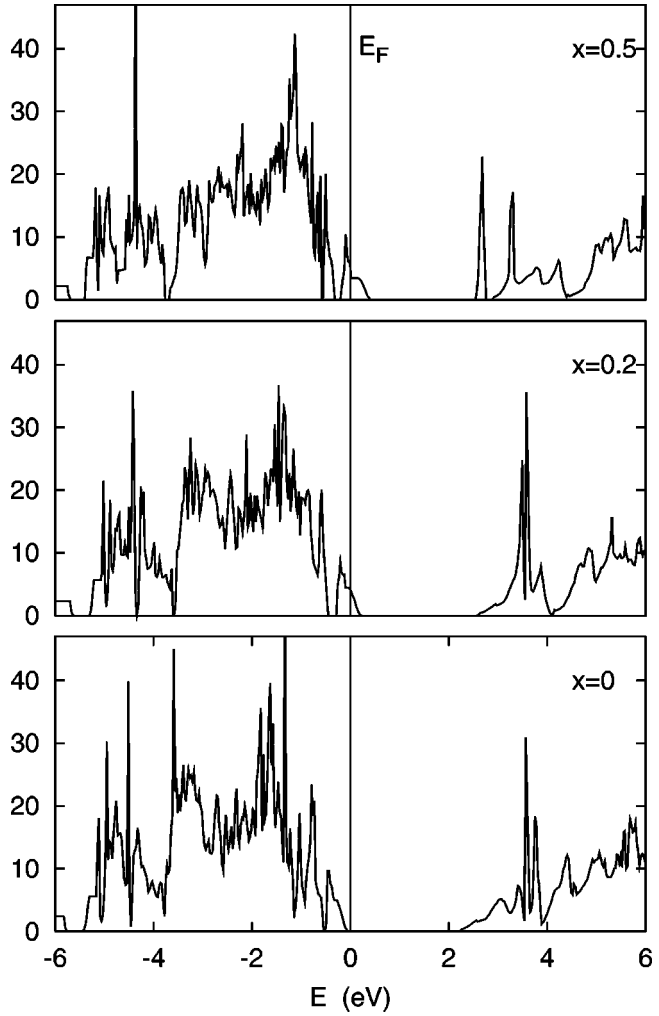

FIG. 9. Same as Fig. 7 but for the LSDA+U^{DFT} method.

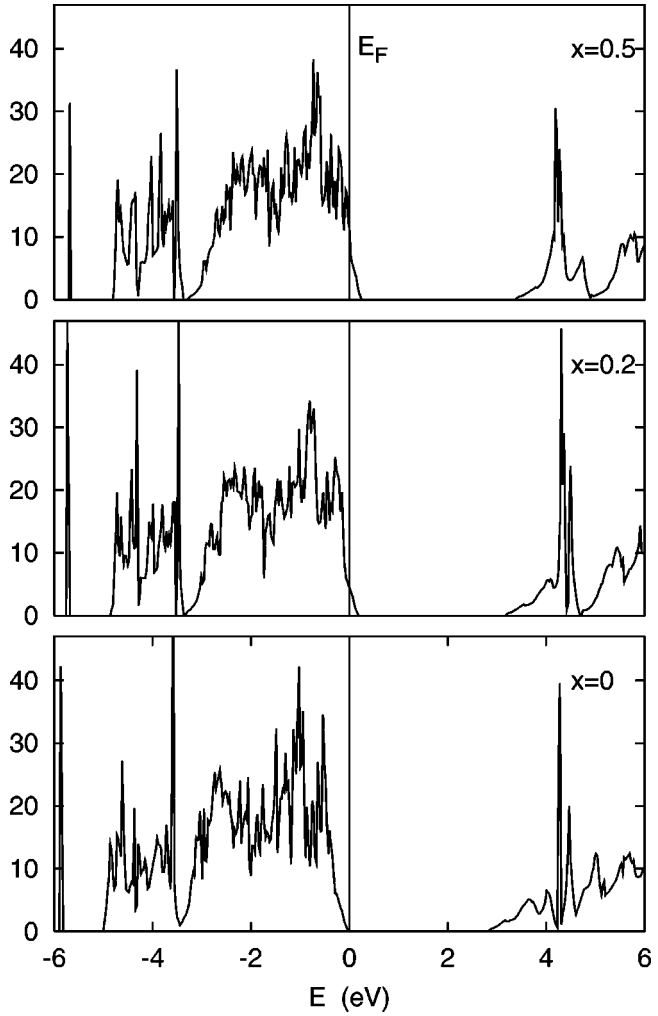

FIG. 10. Same as Fig. 7 but for the LSDA+U^{SIC} method.

23% of O1 $2p_z$, 20% of O2 $2p_x$, and 8% of O2 $2p_y$ character. These fractions depend to some extent on the radii of the atomic spheres, but the qualitative picture is clear—the band can be associated with the strongly hybridized, antibonding Ni($3d_{z^2}$)-O($2p$) band. While the significant fraction of the p_z state of the O1, which lies in the Ni-O-Ni chain, is expected, it is interesting that there are also comparable fractions of the p_x and p_y states of O2, which are situated in the planes perpendicular to the chains. Similar situation exists also for the band structure calculated by LSDA and GGA, but LSDA+U^{SIC} method leads to different result, as there are more bands intersecting the Fermi level. Even in this method the above situation is regained, however, if U and J are scaled. The distribution of the electron density in the NiO_6 octahedron, which corresponds to the first unoccupied band in the Z point of the Brillouin zone is displayed in Fig. 13 (LSDA+U^{DFT} method employed).

A simple way to explain the evolution of the cell parameters is to discuss it in terms of the Ni-O distances. In fact, compared to the parent compound, a shortening of the Ni-O distances is expected for the substituted compounds as some electrons have been removed from the top of the antibonding band.[20] In other words, the decrease of the Ni-O distances leads to an increase of the Ni($3d_{z^2}$)-O($2p$) hybridization and, as a consequence, the partially filled antibonding states are pushed up. At the same time, corresponding fully occupied bonding states are pushed down. There is thus a gain in the total energy of the electronic system, which explains the experimental fact that all the Ni-O distances decrease when concentration of M is increased.[5] The electronic pressure is then strong enough to decrease the unit-cell parameters c (both M=Ca,Sr) and a (Ca only), while in the remaining cases the effect of larger radii of M^{2+} ions prevails.

C. X-ray absorption

The oxygen K-edge x-ray absorption (transitions from $1s$ to p oxygen states) in the $Y_{2-x}M_xBaNiO_5$ system was studied by DiTusa *et al.*[3] and by Lannuzel *et al.*[20] Experimental spectrum of the parent compound consists of a broad peak at $\approx$535 eV with a partially resolved peak A at $\approx$531 eV. Doping by Ca or Sr has only little effect on these two features, but a new, relatively weak peak B appears at $\approx$528 eV. It is natural to associate the new peak with the pocket of the empty states that exists in the substituted systems just above the Fermi level (Figs. 7–10). Indeed the

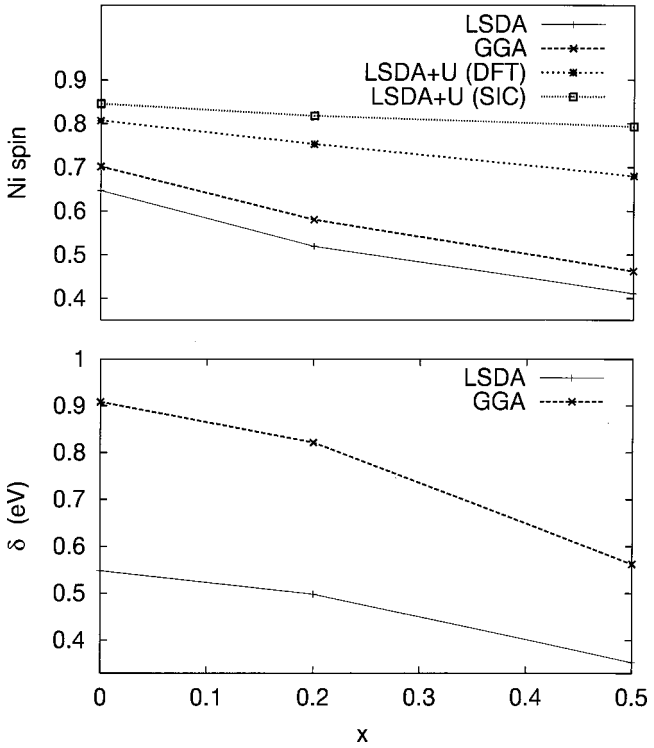

FIG. 11. $Y_{2-x}M_xBaNiO_5$. Dependence of the spin of Ni and of the energy difference δ between antiferromagnetic and nonmagnetic state on the content of *M*.

simulation of the oxygen *K*-edge x-ray absorption spectrum using the LSDA+U^{DFT} results in a good agreement with the experiment (Fig. 14), as far as the relative positions of the peaks are concerned. The peak *A* arises from strongly intermixed Ni 3*d* and O 2*p* states situated ≈ 3.5 eV above the Fermi energy, while the higher broad peak originates from the transitions to states that have predominantly yttrium and barium character. The simulation based on the LSDA+U^{SIC}

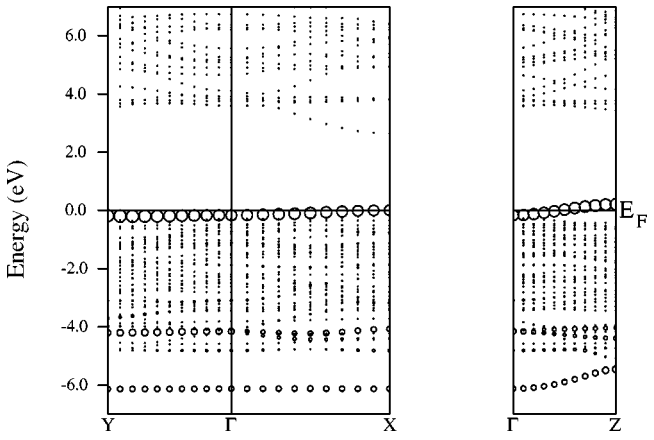

FIG. 12. $Y_{1.8}M_{0.2}BaNiO_5$. The electron band structure calculated by the LSDA+U DFT method. The character of the Ni 3*d* spin-up z^2 states is indicated by the radius of the circles. In the Brillouin zone corresponding to the orthorhombic structure (Ref. 1) the special points have the co-ordinates X=(1,0,0), Y=(0,1/2,0), Z=(0,0,1/2).

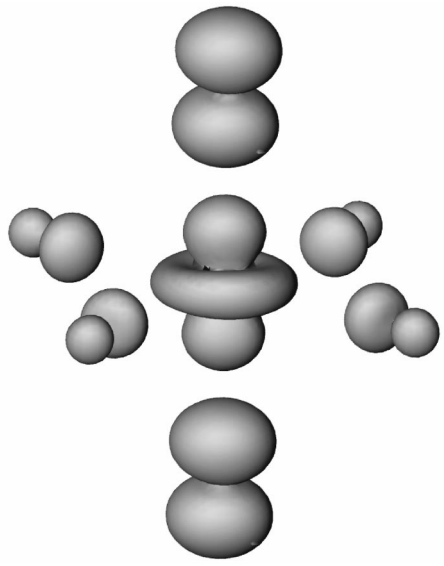

FIG. 13. $Y_{1.8}M_{0.2}BaNiO_5$. The electron-density distribution in NiO_6 octahedron as calculated by the LSDA+U DFT method corresponding to the first unoccupied band in the *Z* point of the Brillouin zone.

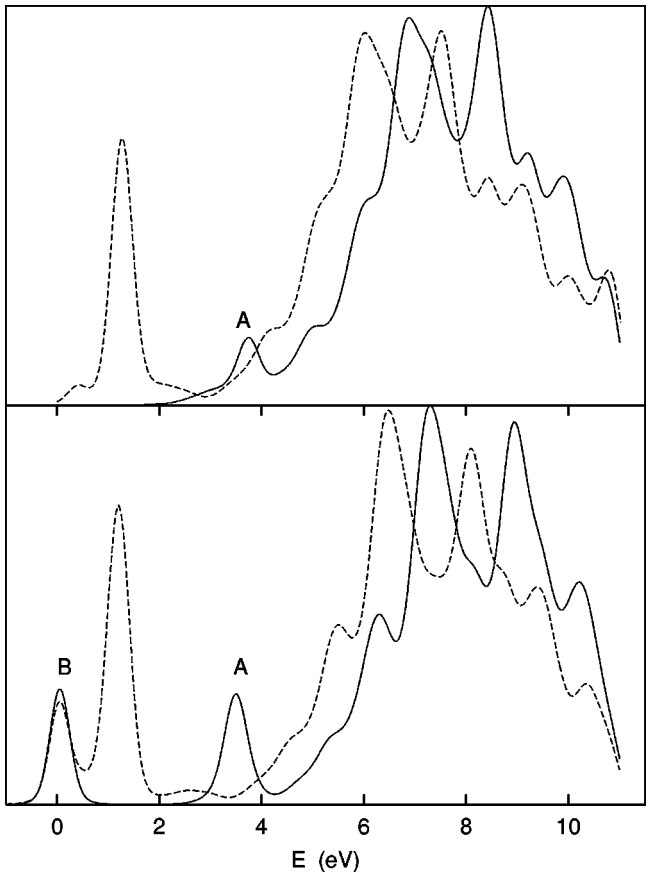

FIG. 14. The oxygen *K*-edge x-ray absorption spectrum of the parent compound (upper panel) and of the $x=0.2$ compound (lower panel). Full and dashed curves correspond to LSDA+U DFT and LSDA methods, respectively.

method yields similar spectrum, but with a larger energy difference between the *A* and *B* peaks, pointing to a need of *U* reduction if this method is used. As for the gap, we estimate that the *U* reduction by $\approx 20-30$ % would bring agreement with the experiment similar to that found for LSDA+U^{DFT}. The simulation based on LSDA and GGA yields the spectra that differ strongly from those observed, as illustrated in Fig. 14 for the LSDA method.

There is one interesting conclusion, which may be deduced from the comparison between the experiment and the calculation—the substitution has little effect on the values of the parameters *U* and *J*. This follows from the fact that the energy difference between the peaks *A* and *B* is rather insensitive to *x* (a remnant of the peak *B* exists also in the experimental spectrum of the parent compound, where it is probably connected with a slight oxygen nonstoichiometry of the sample). On the other hand, as seen in Fig. 5, the position of the peak in the density of states, which corresponds to the peak *A* depends strongly on *U* and *J*.

IV. CONCLUSIONS

From the preceeding sections, it follows that the LSDA+U methods describe the electronic structure of the $Y_{2-x}M_x BaNiO_5$ system better, compared to more conventional LSDA and GGA. On the other hand, the results obtained do not allow us to make the conclusion which of the two LSDA+U variants should be preferred. While LSDA+U^{DFT} yields correct gap and x-ray absorption spectra with the values of parameters *U* and *J* adopted from NiO, LSDA+U^{SIC} would give similar good results if these parameters are reduced by $\approx 20-30$ %. It is dangerous, however, to generalize this conclusion, i.e., to assume that LSDA+U^{DFT} is equivalent to LSDA+U^{SIC} with reduced *U* and *J*. The additional potential of the LSDA+U methods is large, typically of the order of several eV, and the resulting effect of the two LSDA+U versions then depends strongly on the details of the electronic structure of the compound in question.

ACKNOWLEDGMENTS

P.N. thanks the CNRS for financing his stay at the Institut des Matériaux Jean Rouxel. The authors are indebted to H. Eschrig, who suggested the LSDA+U^{DFT} method and to C. Payen, X. Rocquefelte, E. Janod, and F.-X. Lannuzel for helpful discussions. The implementation of the LDA+U method in the WIEN program was supported by Grants No. A1010715/1997 of GA ASCR, 202/00/1602 of GA CR and by the Czech-Austrian Project No. KONTAKT 1999/21.

[1] K. Maiti and D. D. Sarma, Phys. Rev. B **58**, 9746 (1998).
[2] L. F. Mattheiss, Phys. Rev. B **48**, 4352 (1993).
[3] J. F. DiTusa, S.-W. Cheong, J.-H. Park, G. Aeppli, C. Broholm, and C. T. Chen, Phys. Rev. Lett. **73**, 1857 (1994).
[4] Guangyong Xu, G. Aeppli, M. E. Bisher, C. Broholm, J. F. DiTusa, C. D. Frost, T. Ito, K. Oka, R. L. Paul, H. Takagaki, and M. M. J. Treacy, Science **289**, 419 (2000).
[5] V. Massarotti, D. Capsoni, M. Bini, A. Altomare, and A. G. G. Moliterni, Z. Kristallogr. **214**, 205 (1999).
[6] P. Blaha, K. Schwarz, and J. Luitz, *WIEN'97, A Full Potential Linearized Augmented Plane Wave Package for Calculating Crystal Properties* (Karlheinz Schwarz, Vienna, 1999).
[7] P. Novák, J. Kuneš, P. Blaha, K. Schwarz, H. Eschrig, and P. Oppeneer (unpublished).
[8] J. Amador, E. Gutierrez-Puebla, M. A. Monge, I. Rasines, C. Ruiz-Valero, F. Fernandez, R. Saez-Puche, and J. A. Campa, Phys. Rev. B **42**, 7918 (1990).
[9] D. J. Buttrey, J. D. Sullivan, and A. L. Rheingold, J. Solid State Chem. **80**, 291 (1990).
[10] H. Müller-Buschbaum and D. Schlütter, J. Less-Common Met. **166**, 7 (1990).
[11] S. Schiffler and H. Müller-Buschbaumw, Z. Anorg. Allg. Chem. **532**, 10 (1986).
[12] E. Garcia-Matres, J. L. Rodriguez-Carvajal, J. A. Alonso, A. Salinas-Sanchez, and R. Saez-Puche, J. Solid State Chem. **103**, 322 (1993).
[13] J. P. Perdew and Y. Wang, Phys. Rev. B **45**, 13 244 (1992).
[14] J. P. Perdew, K. Burke, and M. Ernzerhof, Phys. Rev. Lett. **77**, 3865 (1996).
[15] V. I. Anisimov, J. Zaanen, and O. K. Andersen, Phys. Rev. B **44**, 943 (1991).
[16] V. I. Anisimov, I. V. Solovyev, M. A. Korotin, M. T. Czyzyk, and G. A. Sawatzky, Phys. Rev. B **48**, 16 929 (1993).
[17] V. I. Anisimov and O. Gunnarsson, Phys. Rev. B **43**, 7570 (1991).
[18] A. B. Shick, A. I. Liechtenstein, and W. E. Pickett, Phys. Rev. B **60**, 10 763 (1999).
[19] W. E. Pickett and D. J. Singh, Phys. Rev. B **55**, 8642 (1997).
[20] F.-X Lannuzel, E. Janod, C. Payen, G. Ouvrard, P. Moreau, and O. Chauvet, J. Alloys Compd. **317-318**, 149 (2001).